

Submillimeter-wave phonon modes in DNA macromolecules

D. L. Woolard,¹ T. R. Globus,² B. L. Gelmont,² M. Bykhovskaia,³ A. C. Samuels,⁴ D. Cookmeyer,¹ J. L. Hesler,²
T. W. Crowe,² J. O. Jensen,⁴ J. L. Jensen,⁴ and W. R. Loerop⁴

¹*U.S. Army Research Laboratory, Army Research Office, Research Triangle Park, North Carolina 27709*

²*Electrical Engineering Department, University of Virginia, Charlottesville, Virginia 22904*

³*Molecular Physiology and Biological Physics, University of Virginia, Charlottesville, Virginia 22904*

⁴*U.S. Army Soldier Biological and Chemical Command, Edgewood, Maryland 21040*

(Received 5 September 2001; published 3 May 2002)

A detailed investigation of phonon modes in DNA macromolecules is presented. This work presents experimental evidence to confirm the presence of multiple dielectric resonances in the submillimeter-wave spectra (i.e., ~ 0.01 – 10 THz) obtained from DNA samples. These long-wave (i.e., ~ 1 – 30 cm^{-1}) absorption features are shown to be intrinsic properties of the particular DNA sequence under study. Most importantly, a direct comparison of spectra between different DNA samples reveals a large number of modes and a reasonable level of sequence-specific uniqueness. This work establishes the initial foundation for the future use of submillimeter-wave spectroscopy in the identification and characterization of DNA macromolecules.

DOI: 10.1103/PhysRevE.65.051903

PACS number(s): 87.15.-v, 87.64.-t, 87.90.+y, 07.57.-c

I. INTRODUCTION

There exists considerable interest in both the experimental and the theoretical investigation of the vibrational dynamics associated with deoxyribonucleic acid (DNA) polymers. Indeed, much effort has been applied to the experimental generation [1–5], and the theoretical interpretation [6–8], of the spectral data originating from the collective electronic mechanics and atomic motions of biopolymers. The underlying motivation for this work is clear. The study of the molecular dynamics, achieved via scattering and absorption spectroscopy, is a viable and proven approach that has been applied widely for the general characterization of molecular conformation [9–11]. Furthermore, there are fundamental physical reasons to expect that an effective application of the spectral data (i.e., especially in the very long wavelength regime) can yield detailed information about complex biological molecules. Since the submillimeter-wave frequency regime (i.e., ~ 0.01 – 10 THz) is predicted to be fairly rich with spectral features that are dependent on DNA internal vibrations that are spread over large portions of the complex molecule [7,12], it is reasonable to expect results that are dependent on the primary sequence of the molecule. Hence, the focus of this work is to investigate the use of submillimeter-wave spectroscopy for the identification and characterization of DNA polymers and to establish a theoretical foundation for future interpretation of phonon modal behavior using THz spectroscopy.

The general need for faster and less expensive techniques that can provide useful structural information leads naturally to spectroscopic techniques that utilize the interaction of an applied electromagnetic (EM) field with the phonon (lattice vibration) field of the material. From the very beginning, Raman spectroscopy has been widely used to provide insight into the three-dimensional structure and microscopic processes associated with biological molecules [2,3]. For example, Raman data provided accurate force constants for theoretical refinements in early lattice-dynamical treatments of

nucleic acid molecules [1,13] and the supporting experimental evidence for “heteronomous” conformations arising in poly(dA)-poly(dT) homopolymers [14]. The Raman effect, which produces frequency shifts in the optical spectra, arises from nonlinear mixing interactions between the naturally occurring phonon modes and those artificially induced by the applied EM field. Hence, Raman scattering results from a second-order optical process and can provide unique information not available from a first-order photon absorption. While Raman scattering is especially effective in the characterization of periodic microstructures (e.g., semiconductors and semiconductor interfaces [15]), it is a very complicated process and correlation between theory and measurement is exceptionally challenging for DNA polymers [16]. In fact, the problem of developing formalisms for the computation of Raman intensities and selection rules in large molecules, such as DNA, has been addressed only recently [17,18]. This fact, combined with the richness of predicted lines in the low-frequency range, has led to an increased interest in the application of submillimeter-wave absorption spectroscopy to biopolymer characterization.

While the application of submillimeter-wave absorption spectroscopy to biopolymers has been somewhat limited to date, indirect techniques such as Raman scattering, the Brillouin scattering, and the neutron scattering have clearly demonstrated standing wave oscillations in DNA polymer chains in the very far infrared (IR) [2,19]. Indeed, most spectral investigations of DNA have been performed at frequencies above 10 THz [5] or towards the higher-frequency portion of the submillimeter-wave domain. The limited number of spectroscopic studies [2,20–23] below this regime may be attributed to the special experimental difficulties that are presented there. In this region between the microwave (~ 100 GHz) and the lower end of the far IR (~ 1000 GHz), the output power of the available sources is limited, the absolute absorption of the biological material is relatively weak, and the high absorption of water masks results from biological materials in solution. These difficulties have severely limited

the direct identification of phonon modes in biological materials at submillimeter-wave frequencies. Investigations performed on dried films of DNA in the 3- to 500- cm^{-1} range have revealed only a few modes. Specifically, work by Witlin *et al.* [21] has found modes of 45 cm^{-1} for the Li-DNA and 41 cm^{-1} for the Na-DNA. Most notable is the observation of four bands near 63, 83, 100, and 110 cm^{-1} in polycrystalline poly(dA)-poly(dT) DNA by Powell *et al.* [2]. While this work did not report any phonon modes below 63 cm^{-1} , it is important to note that the authors believed that “it is not possible to make meaningful measurements at frequencies lower than 40 cm^{-1} because the polynucleotide samples are too fragile to form the sufficiently thick and large diameter films required to provide adequate absorption below 40 cm^{-1} .” Finally, Lindsay and Powell [22] have previously reported a mode in DNA around 12 cm^{-1} and there have been reports of DNA modes in the microwave range (i.e., $<0.3 \text{ cm}^{-1}$) from measurements of DNA solutions by Edwards *et al.* [23]. However, later confirmations and interpretations of these results have not been reported. Hence, previous investigations have not definitively established the existence of DNA phonon modes at submillimeter-wave frequencies below the infrared. Much more recently, new studies on dry DNA samples have suggested that microwave-frequency resonant modes exist that are unique to DNA type and this has been the motivation for the studies presented here [24].

With increased availability of DNA sequence information, as a result of various genomic sequencing projects worldwide, there is a keen interest in determining new methods of extracting primary sequence information for clues to biological and functional properties [13,25]. It is generally accepted that the translational and rotational motions of biopolymer molecules must be related to their properties and biological functions [26]. The desire to understand the mechanisms of DNA function in biological processes has motivated much study of biopolymer dynamics [27]. Previous theoretical studies by Van Zandt and Saxena [12] have predicted that DNA phonons in the intermediate submillimeter-wave range (i.e., 0.01–10 THz) arise out of poorly localized motions that are spread over one or more base-pair units. Here, the dynamics are dominated by interactions of moderate strength and range, which includes the weak hydrogen bonds of the DNA base pairs. Hence, phonon modes that arise in this intermediate range should reflect features specific to the DNA code. Furthermore, theoretical studies have predicted DNA phonon frequencies throughout this regime [28–31] including an optical mode as low as 3 cm^{-1} [31]. Therefore, the scientific motivation for further investigation is exceptionally strong.

This paper presents experimental results on the nature of phonons within the long-wavelength regime. In these studies, detailed transmission measurements were performed on DNA films to search for the occurrence of dielectric resonances in the frequency band from approximately 300 GHz to 100 THz. These results confirm that a portion of the submillimeter-wave spectra (i.e., $\leq 1 \text{ THz}$) contains numerical structures that are unique to the individual biopolymers under investigation. Specifically, dry films of randomly ori-

ented herring DNA sodium salt and salmon DNA sodium salt were investigated and shown to possess large numbers of resonant features. In addition, and most importantly, the individual spectra of the oriented samples were shown to contain features that are sequence specific. This work has confirmed the utility of long-wavelength phonon modes as probes to the structure and dynamics of DNA. Furthermore, this work has laid an important foundation for the application of submillimeter-wave spectroscopy to the area of biological science, medical applications, and in the arena of military defense against warfare agents [25].

II. THE EXPERIMENTAL PROCEDURE

A. Instrumentation

In this study, detailed Fourier-transform infrared (FTIR) spectroscopic investigations of DNA films were performed over the broad spectral range from ~ 10 to 4000 cm^{-1} wave numbers. Here, transmission measurements were performed to determine the material absorption characteristics. These experiments were utilized to search for the occurrence of dielectric resonances induced by interactions of the EM field with long-wavelength phonons. The spectral studies reported on here utilized a commercial Fourier-transform spectroscopy (FTS) (Bruker IFS-66) system. The FTS system is equipped with mercury lamp ($<100 \text{ cm}^{-1}$) and glowbar (100–4000 cm^{-1}) sources, and offers deuterated tri-glycine-sulfate detector (DGTS) (room temperature) and liquid-helium-cooled Si-bolometer ($T=1.7 \text{ K}$) signal detection. The sample chamber of the spectrometer was placed in vacuum to eliminate any influence of water-absorption lines. The resolution was set between 0.2 and 2 cm^{-1} , and up to 512 interferograms were accumulated, co-added, and Fourier transformed. In all cases cited here, baseline correction (graded or uniform shift) was not necessary.

B. Sample preparation and measurement conditions

The investigations reported here considered both uniform and nonuniform films of dry DNA material. In addition, the studies considered randomly oriented and partially aligned DNA chains. It is appropriate to mention here that measurement results are strongly dependent on a number of factors (e.g., sample preparation, humidity, and temperature). Indeed, in order to successfully resolve phonon resonances in biological materials one must consider the effects of interference and mode coupling strength. For example, very uniform solid films are well known to exhibit interference fringes in their reflection and transmission spectra. Furthermore, the interference phenomena can obscure fine resonant features or be misinterpreted as modes themselves [2]. As will be shown, the samples with randomly varying thickness allowed for estimations of the phonon resonances via transmission averaging (see the following section). It should also be noted that the fine structures observed here required spectral resolutions better than 0.5 cm^{-1} . This requirement may partially explain why earlier FTIR investigations were not able to detect them. An equally important point for detection is the optimization of the coupling between the EM field and the dipole moment of the DNA oscillator. As will be shown,

measurements on unoriented dry films result in mode damping and a weak coupling to the EM field. This leads to spectral results where the occurrence of some modes varies from sample to sample. Conversely, spectral results are much more consistent within oriented samples. Specifically, the number and frequency of phonon modes is directly tractable with angle of orientation to the aligned DNA samples. It should be noted that some modes are orientation independent.

The DNA films were prepared by dissolving herring DNA sodium salt (type XIV from herring testes, Lot 14H7121 with 6.5% Na content), and salmon DNA sodium salt (type XIV from salmon testes, Lot 44H7020 with 6% Na content) obtained from Sigma Chemical Co. using glass-distilled water with a concentration ratio between 5:1 and 10:1. The material then formed a gel that was brought to the desired thickness by placing the gel inside an arbor shim between two Teflon films or polycarbonate membranes. The entire mold was left to dry at room temperature in air or in vacuum. The samples were then separated from the entire mold, when possible, to exclude all interference effects and all transmission losses due to the Teflon films. The thinnest samples had good planarity, although they sometimes had an imperfection density (i.e., voids) of about 5–10%. The thickness of the dried films were measured with a Gauge Stand ONO SOKKI ST-022. The drying process typically reduced the sample thickness between two to three times its initial value. All the samples that were considered in this study possessed a final film thickness between 30 and 300 μm .

All measurements were obtained from free-standing films. Films of various thicknesses were utilized to confirm that the observed resonances were directly attributable to the absorption characteristics of the biological material. Interference effects were documented in cases of very uniform films and contrasted to samples with randomly varying imperfections in optical thickness. The mathematical procedure used to derive the dielectric properties for this particular condition of quenched fringes will be fully discussed in the following section.

C. Calculation of refractive index n and extinction coefficient k

The measurements obtained in this paper were used to derive the high-frequency dielectric properties of the biological agents under consideration. Here, the investigation seeks to resolve the frequency-dependent nature of the material that results directly from the microscopic resonant phenomenon. When optically active resonance is present in any material a frequency-dependent, lossy, dielectric characteristic will result. Such a dielectric will exhibit an effective permittivity of the form

$$\varepsilon(\nu) = \varepsilon_{\text{real}} + i\varepsilon_{\text{imag}} = \varepsilon_{\infty} + \sum_j \frac{S_j \nu_j^2}{(\nu_j^2 - \nu^2) - i\gamma_j \nu}, \quad (1)$$

where ε is the complex dielectric function, ν is the frequency in wave numbers, and $\varepsilon_{\text{real}}$ and $\varepsilon_{\text{imag}}$ are the real and imaginary parts, respectively. The last term in Eq. (1) explicitly

gives the complex permittivity in terms of the high-frequency dielectric constant ε_{∞} and a sum over the Lorentz oscillator states. Here, S_j is the oscillator strength, ν_j is the eigenfrequency, and γ_j is the full width at half maximum associated with each harmonic oscillator. The dielectric properties of the films may be equivalently characterized by the complex index of refraction defined by

$$N(\nu) = n + ik, \quad (2)$$

where the real part n is the refractive index and the imaginary part k is the extinction coefficient. In almost all materials (i.e., nonmagnetic) the index of refraction and the dielectric constant are defined according to $N = \sqrt{\varepsilon/\varepsilon_0}$ where ε_0 is the permittivity of a vacuum, hence, the individual terms in Eqs. (1) and (2) are related by

$$\varepsilon_{\text{real}} = n^2 - k^2, \quad (3)$$

$$\varepsilon_{\text{imag}} = 2nk. \quad (4)$$

Lossy dielectrics, with nonzero $\varepsilon_{\text{imag}}$ and k , introduce an exponential damping factor [i.e., $\exp(-\alpha z)$] to the propagating electromagnetic wave in the z direction with an attenuation constant defined by [32]

$$\alpha = \frac{4\pi k}{\lambda_o} = \frac{2\pi\varepsilon_{\text{imag}}}{\lambda_o n}, \quad (5)$$

where $\lambda_o = c/f = \nu^{-1}$ is the wavelength in free space. In theory, if one seeks to derive a frequency-dependent attenuation (or extinction) coefficient from *very* uniform films then the effects of interference must be addressed. Specifically, films that are sufficiently uniform and thin can be expected to exhibit frequency dependence both in their transmission and reflectance spectra due to fringing effects. In this situation, the effects of geometrical interference must be subtracted from the spectra to derive the true frequency dependence of the material parameters. When fringes are observed in measurements, interferometric techniques (i.e., varying wavelength or thickness) must be employed directly to determine the dielectric properties. Furthermore, numerical iterations are necessary to discriminate the natural wavelength dependence of the material from those produced by the geometry of the film [2].

Fortunately, the effects of geometrical fringing can be artificially excluded by precise control of film thickness variations (e.g., lapping in semiconductor film measurement) or naturally diminished by random variations introduced by imperfections. In such situations where fringes are not resolved, an average transmission can be defined and measured that resolves the dependence of the dielectric (or optical) parameters on spectral wavelength. Specifically, the average transmission through a nonfringing film of randomly varying thickness is given by [32]

$$\langle T \rangle = \frac{(1 - R_S)^2 (1 - k^2/n^2)}{\exp(\alpha d) - R_S^2 \exp(-2\alpha d)}, \quad (6)$$

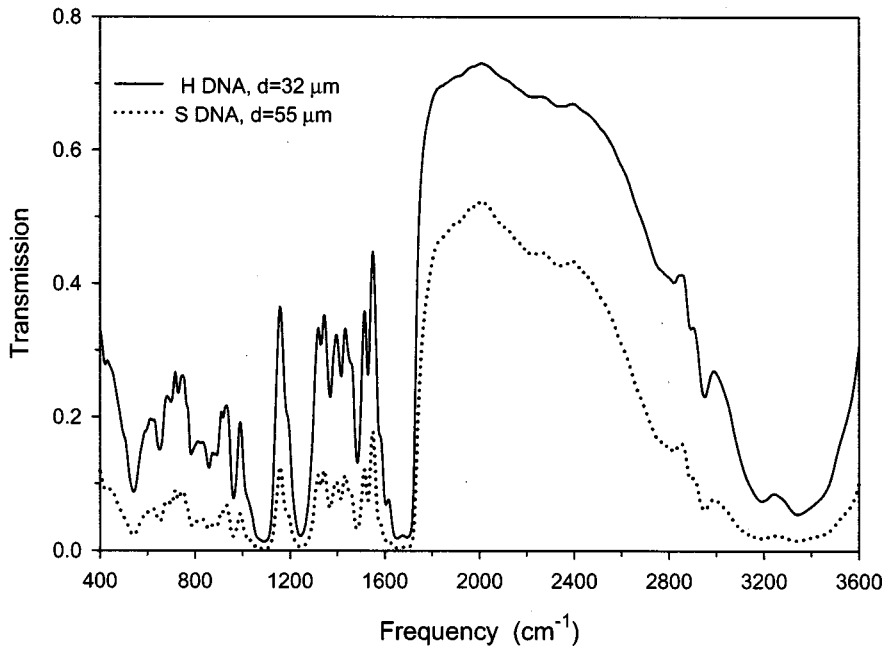


FIG. 1. Salmon and herring DNA transmission spectra taken from a broad sweep over the very far infrared regime.

where d is the average thickness of the film and R_S is the surface reflectance (i.e., of an equivalent air and infinite-film interface) given by

$$R_S = \frac{(n-1)^2 + k^2}{(n+1)^2 + k^2}. \quad (7)$$

If the material is sufficiently lossy such that

$$\exp(2\alpha d) \gg R_S^2, \quad (8a)$$

$$k^2 \ll n^2 \quad (8b)$$

are true, then Eqs. (6) and (7) simplify to

$$\langle T \rangle = (1 - R_S)^2 \exp(-\alpha d), \quad (9)$$

$$R_S = \frac{(n-1)^2}{(n+1)^2}. \quad (10)$$

Data collected for two samples of different average thickness can now be used to eliminate the surface reflectance and define the absorption coefficient as

$$\alpha = \frac{\ln \langle T_1 \rangle / \langle T_2 \rangle}{(d_2 - d_1)}, \quad (11)$$

where $\langle T_1 \rangle$ and $\langle T_2 \rangle$ are the average-transmission measurements for samples of thickness d_1 and d_2 , respectively. Once the transmission and the absorption coefficients have been determined over some frequency band of interest, Eqs. (9) and (10) can be used sequentially to extract the refractive index $n(\nu)$ and Eq. (7) can be used to determine the extinction coefficient $k(\nu)$. The assumptions utilized from Eq. (8) can now easily be verified for accuracy.

In the results reported here, simultaneous measurements of optical transmission through samples of different thickness, prepared under the same conditions, were used to de-

termine the absorption and refractive index spectra. For most of the data presented the effects of specimen imperfections and/or spectral bandwidths were such that the material characteristics were derived using the nonfringing procedure described above. In addition, the materials studied possessed sufficient loss to justify the use of Eqs. (9) and (10). This procedure allowed for the interrogation of narrow spectral features in the dielectric characteristics.

III. MEASUREMENTS RESULTS

FTIR spectroscopic studies were performed over a very broad frequency region (i.e., $\sim 10\text{--}4000\text{ cm}^{-1}$) that encompassed the major portion of the very far infrared spectrum where optically active phonon phenomena are expected. It should be noted (see the following section) that the elastic nature of DNA polymers results in structural vibrations that are acoustic modes below approximately 0.01 THz (0.3 cm^{-1}). Hence, DNA phonon modes in the microwave and millimeter-wave regime, with wavelengths greater than 3 mm, are for the most part optically inactive and absorption spectrum from this region cannot be expected to yield a great deal of information about the internal structure of the polymer [6]. On the other hand, there are two distinct regions within the submillimeter-wave diapason where phonon modes can be expected to reveal information about the molecular structure of DNA. Above about 10 THz the short-range, covalent bonds of nucleotides present within the DNA polymer are the primary source of the phonon modes. Therefore, similar modes should result whether these nucleotides are isolated or appear as constituent elements inside complex DNA chains. Hence, spectra from different DNA species within this high-frequency regime should not differ greatly. Conversely, in the low-frequency band 0.01–10 THz, the spectral features have been predicted to result from poorly localized motions that are dictated by structural factors from several nearest-neighbor base-pair units. Therefore, phonon

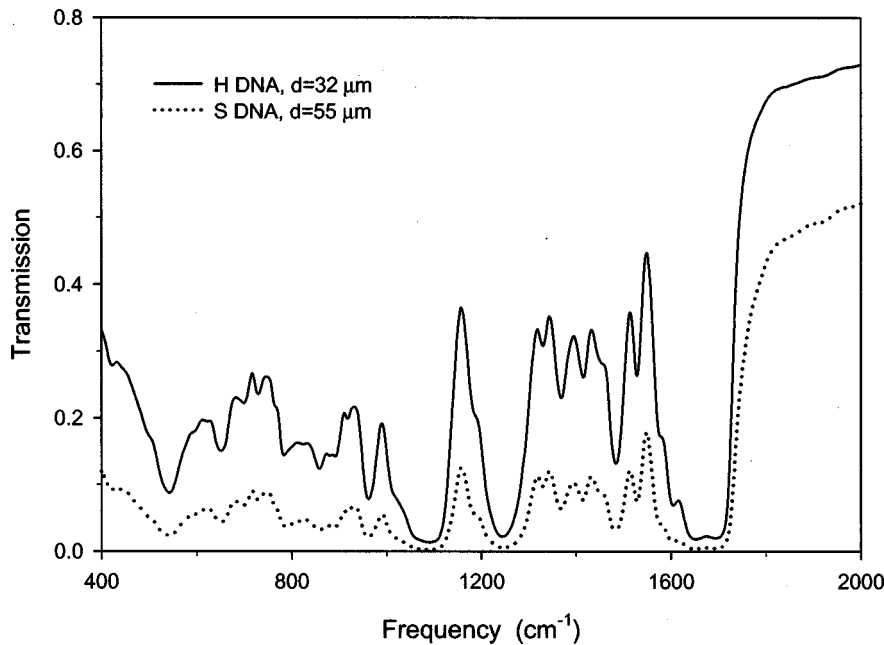


FIG. 2. A comparison of salmon and herring DNA spectra over the terahertz frequency subband.

modes that arise in this portion of the submillimeter-wave regime should reflect features specific to the DNA sequence. The two subsections that follow will present measurement results from each of the optically active spectral regimes and confirm these previous conclusions that were heretofore based almost exclusively on theoretical considerations.

A. High-frequency regime measurements

Detailed FTIR transmission measurements were performed on dry, free-standing, thin-film samples of DNA taken from both salmon and herring testes in the region 400–4000 cm^{-1} . Figure 1 presents a transmission measurement sweep for both salmon and herring samples that shows the majority of the region considered (note that the region above 2000 cm^{-1} lacks interesting features and has been excluded from later results). It should be noted that measurements per-

formed in this high-frequency domain were performed on randomly oriented DNA. Here, heavy absorption and multiple, broad features are present in the high-frequency regime between 400 cm^{-1} and 1800 cm^{-1} . Figure 2 presents a typical set of results and compares the transmission spectra from salmon and herring DNA samples in this same frequency region. These results, which utilized a relatively low-resolution scale of 5 cm^{-1} , reveal that salmon and herring exhibit broad resonances that are in direct agreement.

Multiple spectral scans for herring DNA were taken and used to derive the absorption coefficient that is given in Fig. 3. The peaks in the absorption characteristic may be attributed to phonon modes associated with stretching and bending motion of covalent bonds. In fact, previous spectral studies performed by Sarkar *et al.* [5] have made assignments for some of these absorption bands in nucleic acids. For ex-

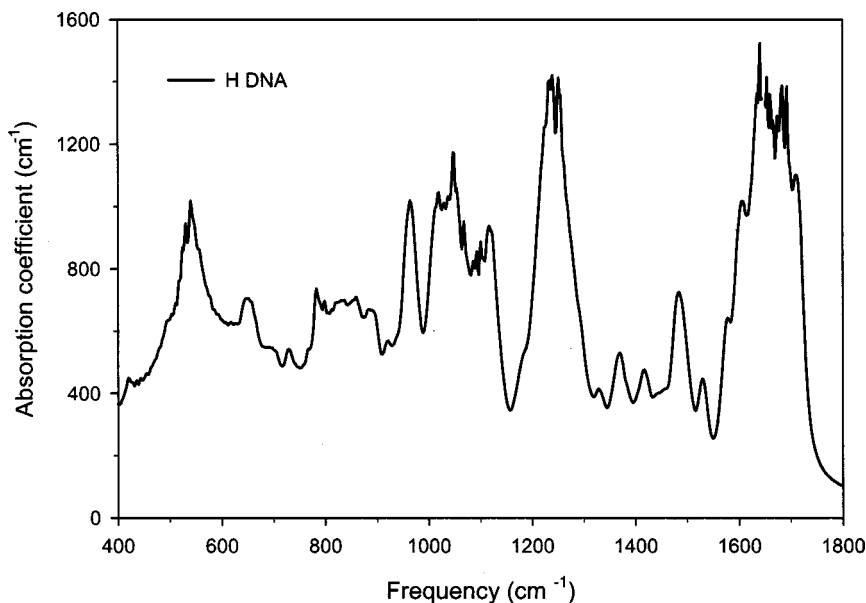


FIG. 3. Absorption characteristics of herring DNA within the terahertz frequency subband.

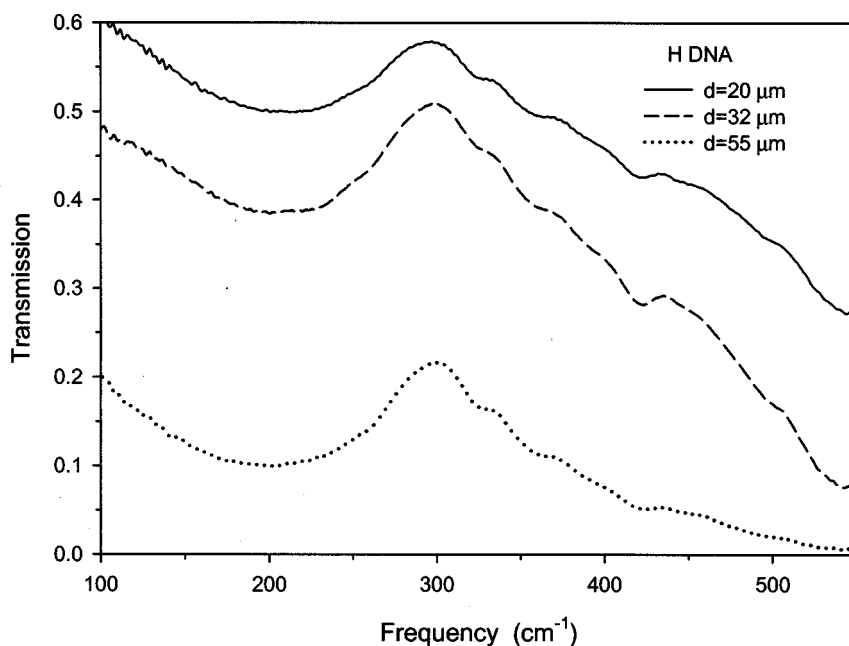


FIG. 4. Herring DNA transmission as a function of film thickness in the upper portion of the submillimeter-wave regime.

ample, these earlier FTIR spectral studies of both DNA and RNA oligonucleotides have documented broad spectral bands in this high-frequency region. In particular, the FTIR spectrum of the 23mer-merDNA hairpin at a temperature of 15 °C shows three bands between 1700 and 1630 cm^{-1} . Our *low-resolution* results show a very broad resonance overlapping these bands at 1692, 1665, and 1644 cm^{-1} . The results of Sarkar *et al.* results assign these peaks to carbonyl stretching vibrations with contributions of the C2=O2 of thymines, C4=O4 stretching vibrations of thymines with contributions C2=O2 of cytosines, and C=C, C=N ring vibrations of thymines engaged in Watson-Crick base pairing. Another example of general mode agreement is the broad peak exhibited at approximately 1080 cm^{-1} in the results of Fig. 3, which has been observed by earlier FTIR

studies [5] of double-stranded RNA oligomers (i.e., 7-mer and 23-mer RNA's). Here the $\sim 1080 \text{ cm}^{-1}$ band is attributed to symmetric PO_2^- stretching mode coupled with the C5'-O5' vibration.

It should be noted that this work cited earlier (i.e., Ref. [5]) for comparison purposes had quite different goals. In particular, these earlier FTIR studies measured high-resolution spectra of RNA and DNA oligonucleotides in D_2O solutions and varied the temperature to detect changes in the molecular conformation. While this earlier work utilized higher-quality samples, performed measurements on nucleic acid solutions, and utilized higher spectral resolution, a comparison of their results to those presented here is very useful for illustrating some important points. First, it demonstrates that phonons arising from the influence of small constituent

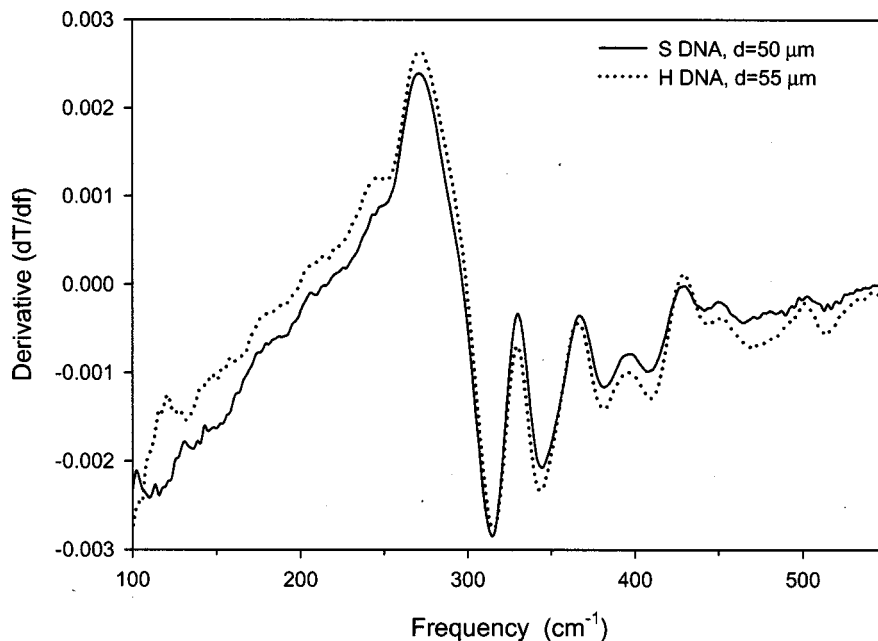


FIG. 5. Differential plot of the transmission characteristic for salmon and herring DNA in the upper portion of the submillimeter-wave regime.

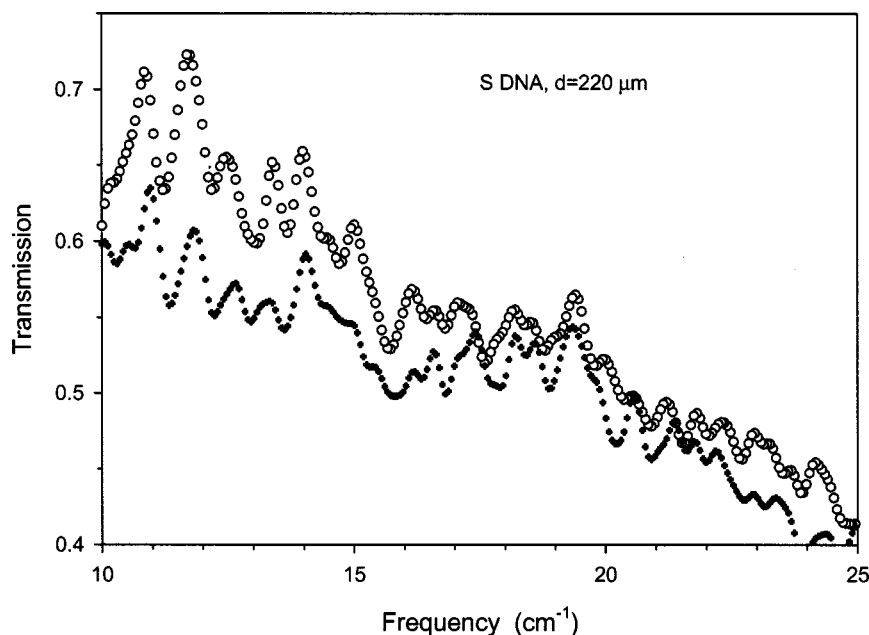


FIG. 6. Two independent transmission measurements of salmon DNA in the lower portion of the submillimeter-wave regime.

molecules can be detected in thin, dry films of DNA as expected. In addition, it further illustrates that these features tend to be somewhat independent of base-pair sequence. Finally, it lends support to the general accuracy and validity of the results from our investigations. In the section that follows, more detailed spectroscopic studies of these DNA samples will be presented that illustrate the utility of submillimeter-wave spectroscopy for the detection and identification of biological agents and for the detailed interrogation of molecular structure. Here, higher resolution will be employed to reveal lower-frequency regime features and how they vary between DNA samples. Furthermore, the results will demonstrate an important dependence on the relative orientation of the DNA samples and the incident EM field.

B. Low-frequency regime measurements

High-resolution FTIR transmission measurements were performed on dry, free-standing, thin-film samples of DNA taken from both salmon and herring tests in the region 10–600 cm^{-1} . To begin let us consider the results obtained from the upper portion of this frequency band between 100 and 600 cm^{-1} . In general, the transmission spectra obtained in this regime above 3 THz in frequency exhibited features that were in very good qualitative and quantitative agreement with previous investigations by others on DNA films (see analysis in [33]). For example, Fig. 4 presents a set of transmission measurements, at 2 cm^{-1} resolution, for varying thicknesses of randomly oriented herring DNA, which indicate resonant-absorption peaks at 212, 424, and 545 cm^{-1} . Figure 5 contrasts differential plots of the transmission characteristic versus wave number (i.e., $\partial T/\partial f$ calculated from smoothing over nine data points) from randomly oriented samples of herring and salmon DNA. Here, approximately similar results for the two different samples are observed. Furthermore, the differential plots reveal a large number of weak shoulder features in the transmission characteristics

over the range 300–600 cm^{-1} . These features are actually soft phonon modes that are obscured by the absorption roll offs from the very strong resonance at 545 cm^{-1} . These experimental results show that all clearly resolvable phonon modes are present in both samples. Hence, this shorter-wavelength portion of the low-frequency regime does not provide signature features for discriminating between samples. However, it should be noted that features in the differential plots are extremely weak between 100 and 300 cm^{-1} and difficult to distinguish.

The manifestation of resonances in the DNA material above 3 THz in frequency was found to be very sensitive to the sample preparation and is relevant for commenting on here. Specifically, the strength (i.e., the relative height) of the resonant features was dramatically affected by the ratio of water-to-DNA concentration used in the film preparation. For example, the intensity of the differential spectral results from a herring DNA film prepared with an 10:1 water-to-DNA concentration is a factor of 10 stronger than the results from a herring DNA film prepared with a 5:1 concentration [33]. This is a direct indication of the resolvability of the peaks that occur in the absorption spectra. Furthermore, this effects both the hard (i.e., zero crossings) and soft resonances and shows that there is significantly stronger coupling of the electromagnetic energy when the samples are prepared with larger concentrations of water. While the fundamental mechanism responsible has not been identified at this point, it is clear that the oscillator strength (i.e., either the phonon density or polarizability) has been affected by the film formation procedure. This phenomenon and its understanding will have many important ramifications for future studies to resolve the dynamics within intrinsic (isolated) DNA macromolecules. For example, if this effect is related to salinity of the sample (e.g., the DNA samples under study are in fact DNA salts) then the prescription for enhancing the phonon activity is important for interrogating the microscopic physical dynamics. In addition, this mechanism may offer a tool

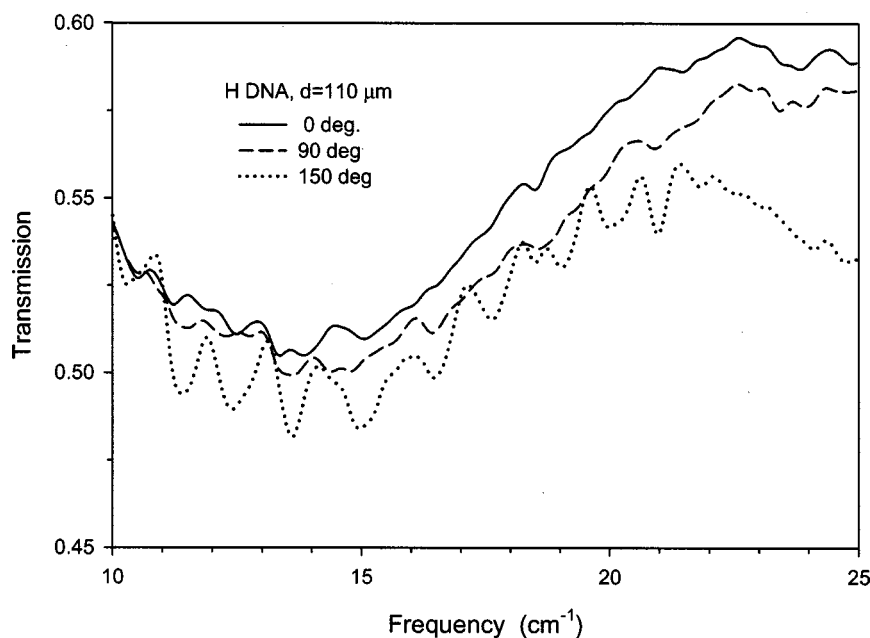


FIG. 7. Transmission spectra for mechanically aligned samples of herring DNA.

for determining the water content associated with DNA samples. Values for the absorption and extinction coefficients were extracted for both herring and salmon films [33] and it is important to note that these results agree very well, both qualitatively and quantitatively, with earlier studies performed by Powell *et al.* [2] on vacuum-dried poly(dG)-poly(dC) DNA. In fact, the values of extinction coefficient for salmon DNA at the transmission window (i.e., ~ 0.04 at 300 cm^{-1}) and at the lower-frequency resonant peak (i.e., ~ 0.105 at 200 cm^{-1}) matched almost exactly with the room temperature measurements on minimal-salt, poly(dG)-poly(dC) films reported on in Ref. [2]. It is appropriate to note that this earlier work considered the influence of salting conditions on various polynucleotides. In fact, they observed

a substantial set of resonances in the band $50\text{--}110\text{ cm}^{-1}$ for minimal-salt Na-poly(dA)-poly(dT) that were strongly dependent on temperature. These resonances were absent in high salt concentration samples. However, the spacing of the relative maxima and minima in the data reported can be explained by thin-film fringing. Specifically, the position of the fringes within their data corresponds almost exactly to a fringing pattern with uniform film thickness $145\text{ }\mu\text{m}$. Hence, it is difficult to tell whether the effects of the salt concentration are macroscopic (i.e., affects the film) or microscopic.

In the very lowest frequency spectral region considered in this study (i.e., $10\text{--}100\text{ cm}^{-1}$) factors arose in obtaining reliable and reproducible experimental data. Specifically, it was observed that the optical characteristics were directly

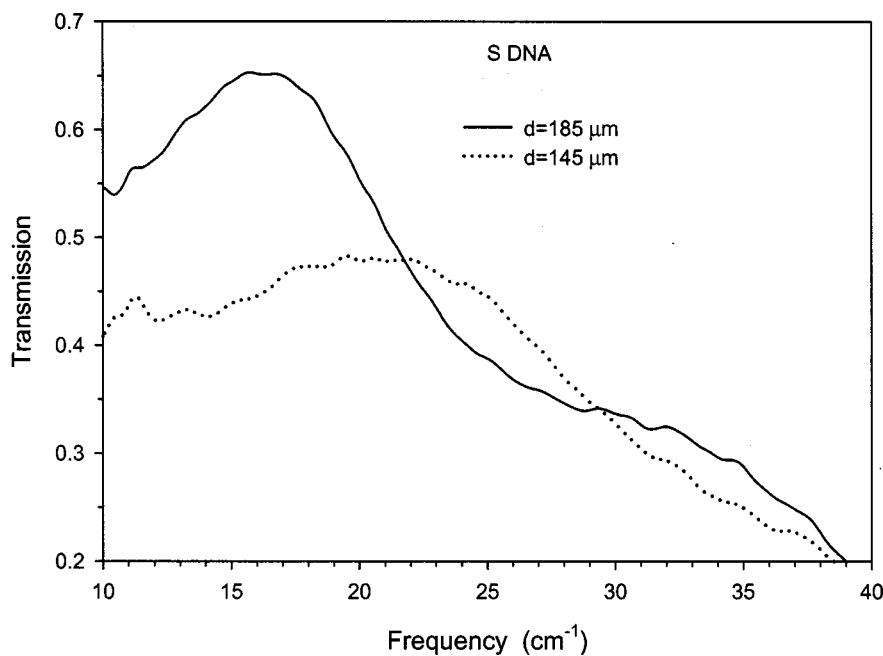


FIG. 8. Transmission spectra taken from salmon DNA films of highly uniform thickness. Note the long-range fringing dependence on film thickness.

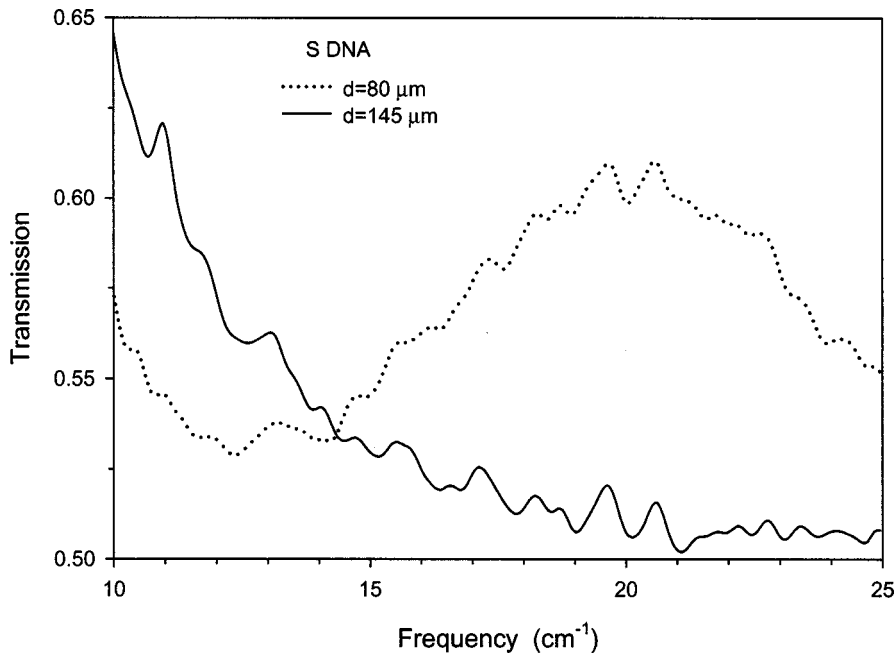


FIG. 9. Transmission spectra taken from mechanically aligned samples of salmon DNA films at the same relative orientation.

dependent on the orientation (i.e., alignment of the DNA fibers) of film samples. Indeed, the mechanical procedures used in sample preparation were observed to influence phonon mode coupling to the measurement field and revealed new details in the fine spectral structure at frequencies below 3 THz. It should first be noted that some DNA samples, as shown in Fig. 6, revealed a large density of resonant features and the high degree of repeatability of the features independent of sample orientation. Note that these initial studies utilized DNA samples that were mechanically aligned by brushing during the film preparation but were measured at random orientations to the measurement field. Furthermore, these type features were observed in both herring and salmon DNA and were clearly due to the material properties of the DNA

sample as was demonstrated by numerous measurements on thin films of various thicknesses [33]. However, further experimentation revealed that there was a variation in some of the spectral peaks on different samples prepared from the same source of DNA. For example, Fig. 7 illustrates results from measurements on a mechanically aligned herring DNA sample at several orientations to the EM field. Here it is easy to observe weak spectral modes (minimum points in the transmission) that both persist (e.g., at approximately 11.5, 12.5, 13.5, and 16.5 cm^{-1}) and vary (e.g., at approximately 17.5, 20.0, and 21.8 cm^{-1}) with sample orientation.

It is appropriate at this time to comment on the general nature of the fine spectral features obtained from the measurements on these DNA samples. It is certainly true that

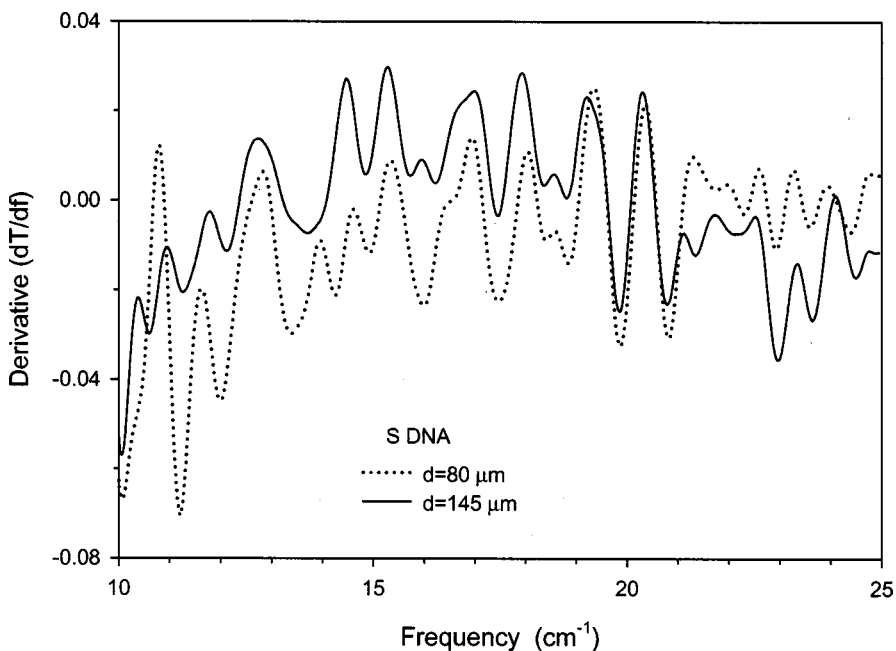


FIG. 10. The differential-transmission characteristics of the salmon DNA film spectral results given in Fig. 9.

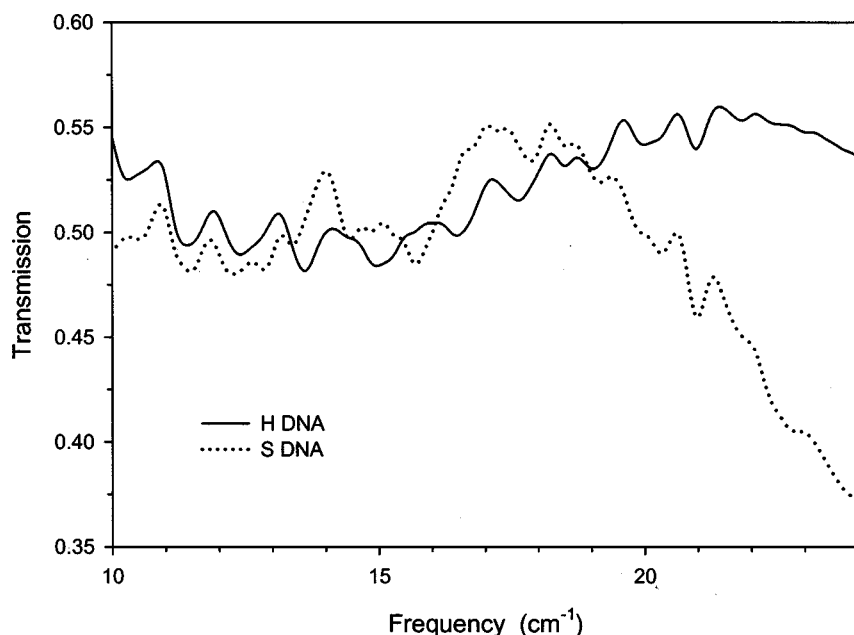


FIG. 11. A comparison of salmon and herring DNA transmission characteristics taken from aligned and identically oriented samples.

these features are relatively weak and in some cases often revealed only as shoulders or inflection points in the transmission results. However, the individual features have variations (i.e., typically of the order of 0.05–0.1) in transmission that are well above noise floor of the FTIR measurement system (i.e., less than 0.01). Furthermore, these features were absolutely stable under repeated measurements. The weak nature of these phonon modes is certainly consistent with expectation. A DNA chain represents a multiple oscillator structure that is not highly periodic in space. Hence, the oscillators contributing to any individual frequency have a low density per unit volume. Therefore, the detection of DNA phonons via resonant absorption is a weak process. Another important factor to note is the influence of the interference effect. In some cases, as in those given in Fig. 6, the natural variations that results over the surface of the film weakens the formation of interference fringes and very distinct phonon modes are revealed. However, for the typical samples considered in these studies (i.e., with $d \sim 200 \mu\text{m}$) the effect of interference fringing in this frequency range manifests itself over many wave numbers [i.e., $\sim (2dn)^{-1} = 20 \text{ cm}^{-1}$ period] as shown in Fig. 8. Since the width of the resonant features are much smaller in extent (i.e., $\sim 0.5 \text{ cm}^{-1}$), there is no direct obscuring of the fine spectra by interference. However, a roll-off of the transmission, as shown in Fig. 8, can transform resonant extrema into shoulders or inflection points in the spectra. Hence, the general agreement of transmission spectra taken from identically prepared salmon DNA samples that were measured at identical orientations, as shown in Fig. 9, is most effectively considered as differential plots, as shown in Fig. 10. As can be seen easily from Fig. 10, there is a very high degree of consistency in the actual and potential (i.e., shoulders and inflection points) resonance modes when mode coupling is optimized through alignment of the oscillator polarization and the EM field. Indeed, the high density of spectral features provides a great deal of information for discrimination of the sample under measurement even over this limited domain from 10 to 25 cm^{-1} . A

direct comparison of aligned herring and salmon DNA samples that were measured at identical orientations is given in Fig. 11. As shown, there are many common phonon modes across the 10–25 cm^{-1} band. However, there are also a number of distinguishing modes in both the herring (i.e., at 15 and 16.5 cm^{-1}) and the salmon (i.e., 12.8 and 15.8 cm^{-1}) spectral plots. Since these measurements were performed on very low quality DNA samples, these results suggest that submillimeter-wave spectroscopy may be a valuable tool for the interrogation of DNA conformation and dynamics. In addition, the observation of polarization effects is important because this is an exact indication of the phonon's dipole moment within the three-dimensional DNA double helix itself.

Therefore, these experimental investigations confirm earlier theoretical studies [7] that predicted a definite relation between the DNA structure and the low-frequency phonon activity. Specifically, earlier studies have pointed out that DNA polymers are of low symmetry and that none of the spectral lines in the very far infrared are truly forbidden. Hence, this low-frequency region should reveal rich spectral features. While this research has confirmed the presence of many low-frequency phonon modes and has identified some unique dynamical features, much more research needs to be done to confirm and understand the nature of this fine structure that has potential application as an important DNA signature.

CONCLUSIONS

A study of phonon mode activity in DNA macromolecules has been presented that confirms the presence of multiple dielectric resonances in the long-wavelength portion of the submillimeter-wave regime (i.e., $\sim 1\text{--}30 \text{ cm}^{-1}$). These experimental results demonstrate the potential of submillimeter-wave spectroscopy as a probe into the primary

sequence, structure, and dynamics of DNA. As shown, when this technique is combined with a robust theoretical capability for the interpretation of the spectral data it has important implications for fundamental biological science, medical applications, and in the arena of military defense against warfare agents.

ACKNOWLEDGMENTS

This work was supported by the U.S. Army Research Laboratory (ARL), the U.S. Army Research Office (ARO), the U.S. Army Soldier Biological and Chemical Command (SBCCOM), and the National Science Foundation (NSF).

-
- [1] G. Maret, R. Oldenbourg, G. Winterling, K. Dransfeld, and A. Rupprecht, *Colloid Polym. Sci.* **257**, 1017 (1979).
- [2] J. W. Powell, G. S. Edwards, L. Genzel, F. Kremer, A. Wittlin, W. Kubasek, and W. Peticolas, *Phys. Rev. A* **35**, 3929 (1987).
- [3] C. Liu, G. S. Edwards, S. Morgan, and E. Silberman, *Phys. Rev. A* **40**, 7394 (1989).
- [4] T. Weidlich, S. M. Lindsay, Qi Rui, A. Rupprecht, W. L. Peticolas, and G. A. Thomas, *J. Biomol. Struct. Dyn.* **8**, 139 (1990).
- [5] M. Sarkar, U. Dornberger, E. Rozners, H. Fritzsche, R. Stromberg, and A. Graslund, *Biochemistry* **36**, 15 463 (1997).
- [6] W. N. Mei, M. Kohli, E. W. Prohofsky, and L. L. Van Zandt, *Biopolymers* **20**, 833 (1981).
- [7] V. K. Saxena, B. H. Dorfman, and L. L. Van Zandt, *Phys. Rev. A* **43**, 4510 (1991).
- [8] Y. Z. Chen, A. Szabo, D. F. Schroeter, J. W. Powell, S. A. Lee, and E. W. Prohofsky, *Phys. Rev. E* **55**, 7414 (1997).
- [9] C. P. Beetz, Jr., and G. Ascarelli, *Biopolymers* **21**, 1569 (1982).
- [10] H. Urabe and Y. Tominaga, *Biopolymers* **21**, 2477 (1983).
- [11] M. Sarkar, S. Sigurdsson, S. Tomac, S. Sen, E. Rozners, B.-M. Sjoberg, R. Stromberg, and A. Graslund, *Biochemistry* **35**, 4678 (1996).
- [12] L. L. Van Zandt and V. K. Saxena, in *Structure & Functions, Volume 1: Nucleic Acids* edited by R. H. Sarma and M. H. Sarma (Adenine, New York, 1992).
- [13] M. B. Hakim, S. M. Lidsay, and J. Powell, *Biopolymers* **23**, 1185 (1984).
- [14] G. A. Thomas and W. L. Peticolas, *J. Am. Chem. Soc.* **105**, 993 (1983).
- [15] L. Bergman, M. Dutta, and R. J. Nemanich, in *Light Scattering in Solids*, edited by R. Merlin and W. Weber (Springer, New York, 1999), Vol. VIII.
- [16] R. Kutteh and L. L. Van Zandt, *Phys. Rev. A* **47**, 4046 (1993).
- [17] R. Kutteh and L. L. Van Zandt, *J. Mol. Spectrosc.* **164**, 1 (1994).
- [18] Y. Z. Chen, A. Szabo, D. F. Schroeter, J. W. Powell, S. A. Lee, and E. W. Prohofsky, *Phys. Rev. E* **55**, 7414 (1997).
- [19] W. K. Schroll, V. V. Prabhu, E. W. Prohofsky, and L. L. Van Zandt, *Biopolymers* **28**, 1189 (1989).
- [20] R. Giordano, F. Mallamace, N. Micali, F. Wanderlingh, G. Baldini, and S. Doglia, *Phys. Rev. A* **28**, 3581 (1983).
- [21] A. Wittlin, L. Genzel, F. Kremer, S. Haseler, A. Poglitsch, and A. Rupprecht, *Phys. Rev. A* **34**, 493 (1986).
- [22] S. M. Lindsay and J. Powell, in *Structure and Dynamics: Nucleic Acids and Proteins*, edited by E. Clementi and R. Sarma (Adenine, New York, 1983), p. 241.
- [23] G. S. Edwards, C. C. Davis, J. D. Saffer, and M. L. Swiscord, *Phys. Rev. Lett.* **53**, 1284 (1984).
- [24] D. L. Woolard *et al.*, *J. Appl. Toxicol.* **17**, 243 (1997).
- [25] D. L. Woolard *et al.*, in *Proceedings of the Fourth Joint Workshop on Standoff Detection for Chemical and Biological Agents*, Williamsburg, VA, 1998.
- [26] T. Shimanouchi, *Pure Appl. Chem.* **36**, 93 (1973).
- [27] R. Beger and E. W. Prohofsky, *Phys. Rev. A* **43**, 5672 (1991).
- [28] B. F. Putnam, L. L. Van Zandt, E. W. Prohofsky, and W. N. Mei, *Biophys. J.* **35**, 271 (1981).
- [29] J. M. Eyster and E. W. Prohofsky, *Phys. Rev. Lett.* **38**, 371 (1974).
- [30] L. Young, V. V. Prabhu, and E. W. Prohofsky, *Phys. Rev. A* **39**, 3173 (1989).
- [31] V. K. Saxena, L. L. Van Zandt, and W. K. Schroll, *Phys. Rev. A* **39**, 1474 (1989).
- [32] T. S. Moss, G. J. Burrell, and B. Ellis, *Semiconductor Optoelectronics* (Butterworths, London, 1973).
- [33] T. Globus *et al.*, in *Proceedings of the International Symposium for Spectral Sensing Research*, Quebec City, Canada, 2001.